Z. Phys. C – Particles and Fields 52, 503–510 (1991)

Zeitschrift für Physik C Particles and Fields

Associate production of a heavy quark and a gauge boson at *ep* colliders

M. Drees[1] and C.S. Kim[2]

[1] Theory Group, DESY, Notkestrasse 85, W-2000 Hamburg 52, Federal Republic of Germany
[2] Department of Physics, University of Durham, Durham DH1 3LE, England

Received 30 April 1991

Abstract. We study the reaction $e+p\to e+Q+V+X$, where Q stands for a c or b quark and $V=\gamma, W$ or Z. At HERA only the combination $Q=c$, $V=\gamma$ seems promising; it should allow to measure the c-quark density inside both the proton and the photon. Here, c-quarks are identified through their muonic decays. At LEP × LHC, $\gamma+b(\bar{b})$ and $W^{\pm}+c(\bar{c})$ production also have sizeable rates; the first reaction might allow to measure the b content of the photon, while the second reaction can determine the strange-sea and the valence d-quark distributions in the proton, and might provide a statistically independent measurement of the $WW\gamma$ vertex.

1 Introduction

The study of final states containing an electroweak gauge boson $V=\gamma, W, Z$ in hadronic collisions has proved very fruitful in the last few years. The production of hard, *isolated* photons [1] is a crucial input for the determination of the gluon density inside the nucleon. The production of W and Z bosons at $p\bar{p}$ colliders [2, 3] has served as important test of the Standard Model (SM) of electroweak interactions [4]. Very recently, the CDF collaboration [5] has begun to use data on W production to constrain valence quark distributions. On the theoretical side, it has recently been pointed out [6, 7] that the interpretation of the results is simplified considerably if the gauge boson is produced in association with a heavy c-quark, which is tagged via its muonic decay. Assuming that the strange sea is known, $W+c$ production [7] gives an unambiguous measurement of the gluon density; $\gamma+c$ [6] and $Z+c$ [7] production can help to determine the presently poorly understood c-quark distribution inside the nucleon.

In this paper we extend these analyses to *ep* colliders. Calculations for the inclusive production of massive vector bosons [8] and hard photons [9] in *ep* collisions exist in the literature, but to our knowledge their associate production with heavy quarks has not yet been discussed. We study $V+Q$ production (for $Q=c, b$) both at the upcoming HERA collider and at the future LEP × LHC collider. We include in our analysis both the "direct" contribution, where the exchanged photons interact directly with the quark inside the proton, and "resolved photon" contributions, where the initial state photon is also resolved into quarks and gluons, which undergo hard scattering off the partons inside the proton. In this way we can obtain information on both the photon and proton structure functions.

The rest of this paper is organized as follows. In Sect. 2 we briefly discuss the necessary formalism, especially the problem of heavy quark densities inside the photon. We also present tables of integrated $V+Q$ events rates for both colliders; we find that at HERA only the combination $V=\gamma$, $Q=c$ offers event rates that allow for a detailed investigation of the reaction. In Sect. 3 we therefore focus on this final state, giving distributions for all relevant kinematical quantities, including the effects of c-quark hadronization and decay; we also discuss the case $Q=b$ for LEP × LHC. In Sect. 4 we study $W+c$ and $Z+c$ production, which is promising only at LEP × LHC and beyond. Finally, in Sect. 5 we summarize our results and present some conclusions.

2 Formalism and total cross sections

We are interested in the leptoproduction of an electroweak gauge boson V and a heavy quark Q. We work in the Weizsäcker–Williams approximation [10], where the cross section for $ep\to QVX$ is expressed as a product of distribution functions $f_{i,j/e,p}$ and a hard scattering cross section $\hat{\sigma}$. Schematically:

$$d\sigma(ep\to VQX)=f_{i/e}(x_e)f_{j/p}(x_p)d\hat{\sigma}(ij\to QV). \tag{2.1}$$

In general, two distinct classes of processes contribute to the production of a given final state, see Fig. 1. In the "direct" process of Fig. 1a the initial-state photon couples directly to a quark inside the proton, i.e. one has $i=\gamma$, $j=q$. We use the leading log approximation for the photon density inside the electron:

$$f_{\gamma/e}(x_e)=\frac{\alpha}{\pi x_e}[x_e^2+(1-x_e)^2]\log\frac{p_T}{m_e}, \tag{2.2}$$

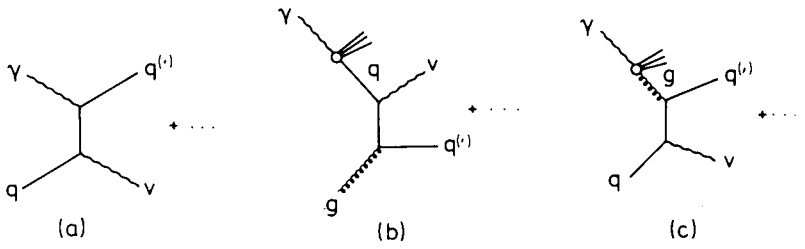

Fig. 1 a–c. Typical Feynman diagrams for the direct **a** and resolved photon **b, c** contributions to the photoproduction of a heavy quark Q and an electroweak gauge boson V. The resolved photon contributions are characterized by the second spectator jet that originates from the remnants of the initial-state photon after a quark (b) or gluon (c) has been extracted from it

where p_T is the transverse momentum of V or Q (which are equal and opposite in our approximation). Our choice of the argument of the log has recently been shown [11] to reproduce exact matrix elements for $e+p\to e+\gamma+$ jet $+X$ quite well. We use standard parametrizations [12, 13] for the parton densities inside the proton, including the heavy quark densities.

In the "resolved photon" processes of Fig. 1b, c, the photon is also resolved into quarks and gluons, which then interact with the partons inside the proton. It has been shown almost 15 years ago [14] that the parton densities inside real photons are $\mathcal{O}(\alpha/\alpha_s)$; the two classes of contributions are thus of the *same* order in coupling constants. The resolved photon contributions can in turn be divided into two subclasses, depending on whether a quark (Fig. 1b) or gluon (1c) is taken out of the photon. In both cases the parton density inside the electron can be computed by convoluting the photon density inside the electron, (2.2), with the parton density inside the photon:

$$f_{q,g/e}(x_e)=\int_{x_e}^{1}\frac{dx}{x}f_{q,g/\gamma}\left(\frac{x_e}{x},Q^2\right)f_{\gamma/e}(x). \tag{2.3}$$

We use the parametrization of [15] for the $f_{q,g/\gamma}(x,Q^2)$. However, this parametrization most likely overestimates the heavy quark content of the photon, since it was obtained by using four or five massless flavours in the evolution equation [16] for all $Q^2>Q_0^2=1\,\mathrm{GeV}^2$. The parametrizations for $N_f=4$ (5) should only be used for $Q^2>20$ (200) GeV^2, but even here the assumption that quark distribution functions only depend on the charge, not on the mass, of the given quark could overestimate the heavy quark densities by a factor of two or more. We therefore also present results where we have modified the $f_{Q/\gamma}$ ($Q=c,b$) according to the prescription of [17]:

$$f_{Q/\gamma}^{\mathrm{mod.\,DG}}(x,Q^2)=f_{Q/\gamma}^{\mathrm{DG}}(x,Q^2)\frac{\log(W^2/4m_Q^2)}{\log(Q^2/\Lambda^2)}, \tag{2.4}$$

with $W^2=Q^2(1/x-1)$. This ansatz correctly reproduces the heavy quark threshold in deep inelastic scattering. The motivation for using this ansatz in timelike processes is somewhat weaker, but it seems reasonable to us that heavy quark structure functions should be less suppressed in the region of small x, as predicted by (2.4). Probably (2.4) is a conservative estimate, since the decrease of the heavy quark contribution to F_2^γ should be compensated by an increase of the light quark densities, in order to reproduce data [18] at large Q^2; since (2.4) relates the distribution functions for light and heavy quarks with given charge, this would also increase the heavy quark densities somewhat. We therefore believe that the true answer lies between the results obtained with the original and modified DG parametrization; probably the modified distributions give more realistic results.

Finally we have to specify the hard scattering cross sections $\hat{\sigma}$. They can be written as

$$\frac{d\hat{\sigma}}{d\hat{t}}(ij\to QV)=\frac{C_{ij}^V}{\hat{s}^2}\frac{\hat{s}^2+\hat{t}^2+2\hat{u}M_V^2}{-\hat{s}\hat{t}}, \tag{2.5}$$

where $\hat{s}=x_e x_p s$ is the squared invariant mass of the $Q+V$ system, $\hat{t}=(p_i-p_Q)^2$, and $\hat{u}=(p_i-p_V)^2$. In the Standard Model, the coefficients C_{ij}^V are given by

$$\begin{aligned}
C_{\gamma Q}^{\gamma}&=2\pi\alpha^2e_Q^4,\\
C_{\gamma Q}^{Z}&=\frac{\alpha e_Q^2G_Fm_Z^2g_Q^2}{\sqrt{2}},\\
C_{\gamma q}^{W}&=\frac{\alpha G_Fm_W^2|V_{qQ}|^2}{\sqrt{2}}\left(|e_q|-\frac{\hat{s}}{\hat{s}+\hat{t}}\right)^2,\\
C_{gQ}^{\gamma}&=\frac{1}{3}\pi\alpha e_Q^2\alpha_s,\\
C_{gQ}^{Z}&=\frac{\alpha_sG_Fm_Z^2g_Q^2}{6\sqrt{2}},\\
C_{gq}^{W}&=\frac{\alpha_sG_Fm_W^2|V_{qQ}|^2}{6\sqrt{2}},
\end{aligned} \tag{2.6}$$

where

$$g_Q^2=\tfrac{1}{2}(1-4|e_Q|\sin^2\theta_W+8e_Q^2\sin^4\theta_W), \tag{2.7}$$

and we have used $\sin^2\theta_W=0.23$. Finally, e_Q and e_q stand for the electric charge of the quarks Q and q, and V_{qQ} is an element of the Cabibbo–Kobayashi–Maskawa quark mixing matrix [19]. Note that m_Q dependent terms have been neglected in (2.5). This is justified since we are only interested in the region $p_T^2\gg m_Q^2$, where the notion of Q-quark distribution functions can be applied. We have, however, kept the m_Q dependence in the phase space.

We are now in a position to present results for total cross sections after cuts. In Table 1 we show predictions for $\gamma+c(\bar{c})$ production at HERA ($E_e=30\,\mathrm{GeV}$, $E_p=820\,\mathrm{GeV}$, $\sqrt{s}=314\,\mathrm{GeV}$). We have added equal c and $\bar{c}$ contributions, and have used $m_c=1.5\,\mathrm{GeV}$. The entries of the first column are for the cuts

$$p_T^\gamma>5\,\mathrm{GeV}, \tag{2.8a}$$

$$|y_\gamma|<4. \tag{2.8b}$$

The cut (2.8a) makes sure that $p_T^2\gg m_c^2$, so that it makes sense to use c-quark distribution functions. The cut (2.8b)

Table 1. Total cross sections after cuts for $\gamma + c(\bar{c})$ production at HERA, for *isolated* photons with $m_c = 1.5$ GeV; the (equal) contributions with c and $\bar{c}$ quarks have been added. In the first column, we only have applied the cuts $p_T^\gamma > 5$ GeV, $|y_\gamma| < 4$, while for the second column we have required the charm (anti)quark to decay into a muon (BR = 0.2) with $p_T^\mu > 2.5$ GeV. The effects of c-hadronization have been included. Direct and resolved photon contributions are shown separately. WWA stands for Weizsäcker–Williams approximation, see (2.2). DG and DGK stand for the parametrization of [15] and its modification [17] according to (2.4)

Process	Structure ftn.	$\gamma + c$ (pb)	$\gamma + c(\to \mu)$(pb)
Direct	WWA ⊗ DO1	8.3	0.20
Direct	WWA ⊗ EHLQ1	2.8	0.09
Resolved	DG ⊗ EHLQ1	25.6	0.52
Resolved	DGK ⊗ EHLQ1	8.7	0.18

on the rapidity of the photon removes events where the photon emerges at an angle of less than 2 degrees to the beam pipe, in which case it would most likely not be detected. Note that we are only interested in *isolated* photons; this removes the potentially large [9] contribution where photons are produced in the fragmentation of quarks of gluons. (In our leading order calculation, $\Delta R^\gamma > \pi$ always, but this will be changed somewhat by parton showers.)

Most probably the c-quark will have to be identified via its decay into a muon, which has a branching ratio of 20%. The entries in the second column give cross sections after the additional cut

$$p_T^\mu > 2.5 \text{ GeV} \tag{2.9}$$

has been applied on the transverse momentum of the muon. We have included c-quark fragmentation using the standard Peterson fragmentation functions [20], which softens the muon spectrum considerably. The $c \to \mu$ decay has been treated in the collinear approximation, which works well in the given case $p_T^2 \gg m_c^2$.

The results of this table show that the $\gamma + c(\bar{c})$ final state is sensitive to the c-quark densities both in the proton (DO1 vs. EHLQ1) and the photon. In a full HERA year of 200 pb^{-1} we expect at least 15 (30) direct (resolved photon) events, where charm is tagged by hard muons. Unfortunately, this is the only of our processes which offers some promise at HERA. The total $W + c(\bar{c})$ cross section with $p_T^W > 5$ GeV is only about 0.06 pb, and the cross sections for $W + b$ and $Z + c$ production are even smaller. Finally, once we apply the cut $p_T^b > 15$ GeV in order to guarantee that $p_T^2 \gg m_b^2$, the cross section for $\gamma + b$ final states is down to 0.09 pb.

Final states containing b quarks or heavy vector bosons, but not both, can, however, be studied at the LEP × LHC collider ($E_e = 50$ GeV, $E_p = 8$ TeV, $\sqrt{s} = 1.3$ TeV, $L = 10^3$ pb^{-1} yr^{-1}). In Table 2 we present results for the $\gamma + c(\bar{c})$ and $\gamma + b(\bar{b})$ final states. For both cases we have required the cuts

$$p_T^\gamma > 15 \text{ GeV}, \tag{2.10a}$$

$$|y_\gamma| < 5, \tag{2.10b}$$

so that once again $p_T^2 \gg m_Q^2$ (2.10a); furthermore, we have

Table 2. Total cross sections after cuts for $\gamma + c(\bar{c})$ (Col. 1) and $\gamma + b(\bar{b})$ (Col. 2) production at LEP × LHC, for *isolated* photons. We have used $m_b = 5$ GeV and applied the cuts $p_T^\gamma > 15$ GeV, $|y_\gamma| < 5$. Notation is as in Table 1

Process	Structure ftn.	$\gamma + c(\bar{c})$(pb)	$\gamma + b(\bar{b})$(pb)
Direct	WWA ⊗ EHLQ1	1.4	0.018
Resolved	DG ⊗ EHLQ1	5.7	0.44
Resolved	DGK ⊗ EHLQ1	2.9	0.13

Table 3. Total cross sections after cuts for $W, Z + c(\bar{c})$ production at LEP × LHC, for $p_T^{W,Z} > 10$ GeV, $|y_{W,Z}| < 5$. Notation is as in Table 1. The resolved photon contribution to cW^- production is practically equal to that to $\bar{c}W^+$ production, since the contribution with a gluon from the photon and a d-quark from the proton is negligibly small

Process	Structure ftn.	$V + c(\bar{c})$(pb)
Direct ($\bar{c}W^+$)	WWA ⊗ DO1	1.1
Direct ($\bar{c}W^+$)	WWA ⊗ EHLQ1	0.78
Resolved ($\bar{c}W^+$)	DG ⊗ EHLQ1	0.06
Direct (cW^-)	WWA ⊗ DO1	1.2
Direct (cW^-)	WWA ⊗ EHLQ1	0.88
Direct (Zc)	WWA ⊗ DO1	0.075
Direct (Zc)	WWA ⊗ EHLQ1	0.036
Resolved (Zc)	DG ⊗ EHLQ1	0.093
Resolved (Zc)	DGK ⊗ EHLQ1	0.040

increased the range of rapidity of the photon (2.10b) in order to take into account the even more asymmetric nature of this collider. We do not show results where we require the heavy quarks to decay into muons. For the case of c-quarks, the reduction factor would be very similar to those at HERA, for a given ratio p_T^μ / p_T^γ, but depends quite sensitively on this ratio. It is at present not clear how hard a muon would have to be in order to be identified in a LEP × LHC collider. The branching ratio for $b \to \mu$ is only about 11%; however, a strong case has recently been made [21] for good b-quark identification using microvertex detectors, which might allow one to detect or rule out an intermediate mass Higgs boson at this collider.

Finally, in Table 3 we show results for the $\bar{c}W^+$, cW^- and $Zc(\bar{c})$ final states. Even after the cut $p_T^V > 10$ GeV we find quite large rates for direct $W + c(\bar{c})$ production, which is sensitive to the $WW\gamma$ vertex. The resolved photon contribution to this final state, as well as total rates for $Z + c(\bar{c})$ production, should still be large enough to at least allow for their detection.

In the next two sections we discuss the most promising final states, $\gamma + Q$ (Sect. 3) and $W, Z + c$ (Sect. 4), in more detail.

3 The $\gamma + Q$ final state

We begin with the reaction $ep \to e\gamma cX$ at HERA. In Fig. 2a, b we show the transverse momentum spectrum and rapidity distribution of the produced photon with the cuts (2.8a, b). The solid curves show the direct contribution (see Fig. 1a), for two different choices for the

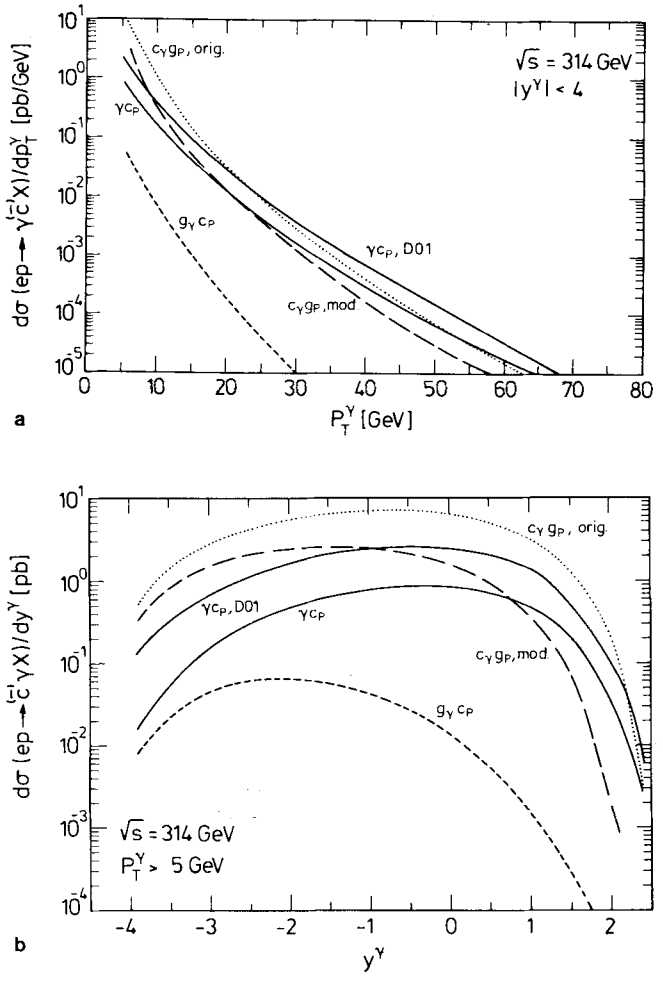

Fig. 2 a, b. The transverse momentum **a** and rapidity **b** distribution of the photon in $\gamma + c(\bar{c})$ events at HERA. The solid curves show predictions for the direct contribution, while the dashed and dotted curves depict resolved photon contributions. We have used EHLQ1 structure functions for the proton, except for the upper solid curves where the DO1 parametrization has been used. The dashed (dotted) curves have been obtained using the modified (original) DG structure functions for the photon, as described in the text. The lower dashed curves show the contribution from the subclass of resolved photon processes depicted in Fig. 1c. We have used $Q^2 = p_T^2$ for the momentum scale both in α_s and in all structure functions and $N_f = 4$ active flavors

c-quark density inside the proton, according to the DO1 [12] (upper) and EHLQ1 [13] (lower) parametrizations. The DO1 parametrization predicts rates that are more than twice the rates predicted by the EHLQ1 parametrization. Figure 2b shows that the excess is especially pronounced in the region of large x_p, which in our convention corresponds to large, negative y. On the other hand, Fig. 2a shows that the difference between the two parametrizations becomes smaller at higher p_T, i.e. higher Q^2. This explains why the reduction of the signal that results when one requires the c-quark to decay into a hard muon is less for the ELHQ1 parametrization, see Table 1.

The dashed curves in Fig. 2 correspond to the two subclasses of resolved photon contributions. The upper curves correspond to the situation depicted in Fig. 1b, where a c-quark from the photon reacts with a gluon from the proton, while the lower dashed curves show the contribution from the subclass depicted in Fig. 1c, where the gluon is taken from the photon and the c-quark from the proton. These curves have been obtained using EHLQ1 structure functions for the proton and modified (see (2.4)) DG structure functions for the photon. (Of course, the modification only affects the contribution where the c-quark is taken from the photon.) We see that the contribution of the subclass of processes depicted in Fig. 1c is entirely negligible everywhere; the reason is that both the gluon density inside the photon and the c-quark density inside the proton are very soft. We can, at present, not exclude the possibility that our choice of structure functions underestimates both these distribution functions by as much as a factor of 2–3 [22]; but even for the most optimistic choice the subclass of Fig. 1c would contribute less than 10% of the total resolved photon events. We can therefore safely conclude that the resolved photon production of the $\gamma + c$ final state is essentially only sensitive to the gluon density inside the proton and the c-quark density inside the photon. Presumably the former will be measured at HERA using different reactions [23], e.g. heavy flavor production; note that we only need it in the region $x_p \geqq 10^{-3}$ if we restrict ourselves to the region $y_\gamma < 1$ where the resolved photon processes dominate. Our reaction would then allow for an essentially unambiguous measurement of the c-quark density inside the photon. In order to demonstrate the present uncertainty in this quantity, we also show predictions using the original DG parametrization (dotted curves). We observe large differences at positive y_γ, corresponding to large x_e and hence small W^2, see (2.4); for very negative y_γ the differences are much smaller. We thus conclude that this reaction can probe both the shape and the normalization of the c-quark density inside the photon.

In order to fully exploit this potential, it will, however, be necessary to distinguish between the direct and resolved photon contributions, since otherwise one would have to determine two unknown functions (the c-quark distributions inside the photon and proton, respectively) with only one data set. Figure 2a shows that one could suppress the resolved photon contributions by going to large p_T^γ; however, then the total cross section is also very small. The rapidity distribution of Fig. 2b offers a better handle; by focussing on small (large) y_γ, one can enhance (suppress) the resolved photon contributions relative to the direct ones. However, in view of the present uncertainties it is not clear whether there is a sizeable region where either contribution is clearly dominant. One will thus probably have to make use of the spectator jet from the photon, which is a unique feature [24] of resolved photon events.

So far we have not specified how the c-quarks are to be identified. By far the most straightforward method of c-quark tagging in a hadronic environment is to look for their decay into muons, which gives a muon inside a jet. Figure 3a, b correspond to Fig. 2a, b when we require the transverse momentum of the muon to be larger than 2.5 GeV. This requirement reduces the signal by about a factor of 8, in addition to the loss of a factor 5 due to the 20% muonic branching ratio of the c-quark, since the μ has typically only 1/3 of the energy of c-flavored hadron,

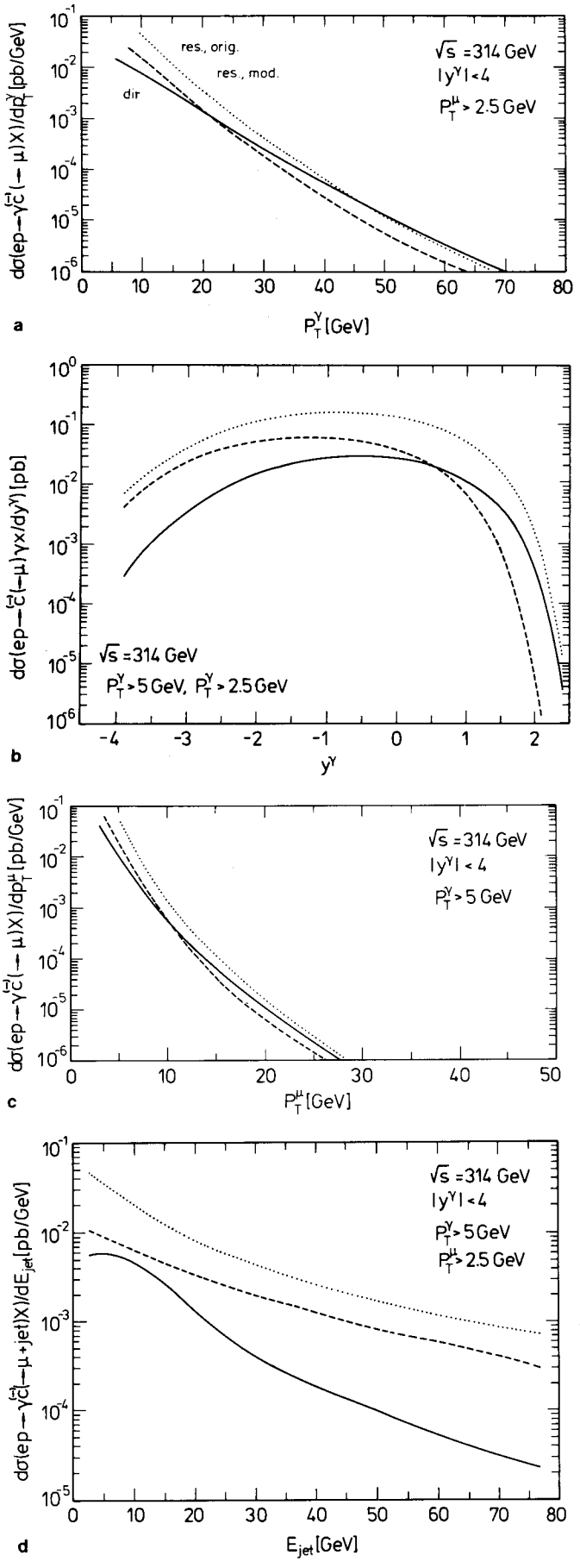

Fig. 3a–d. Characteristics of $\gamma + c(\bar{c})$ events at HERA when the c (anti)quark is tagged by a muon with $p_T^\mu > 2.5\,\text{GeV}$. We show the transverse momentum **a** and rapidity **b** distribution of the photon, the transverse momentum spectrum of the muon **c** and the energy spectrum of the c-jet **d**; the latter gets contributions both from c-quark fragmentation and decay. EHLQ1 structure functions have been used for the proton. Other parameters and notation are as in Fig. 2

which in turn carries on the average only a bit more than 50% of the energy of the original c-quark. The absolute size of our signal thus depends quite sensitively on this cut. However, we see that the shapes of the p_T^γ and y_γ distributions are not much altered, so that our conclusions drawn from Fig. 2 are still valid. If direct and resolved photon contributions can be distinguished on an event-by-event basis, we see that for our choice of cuts one full HERA year, corresponding to an integrated luminosity of $200\,\text{pb}^{-1}$, should suffice to give significant new information on the size of the c-quark distribution functions for both the photon and the proton. For a more detailed study of the shapes of these distributions one would probably need a larger data sample, unless our p_T^μ cut can be somewhat relaxed.

In Fig. 3c, d we show the transverse momentum spectrum of the μ and the energy spectrum of the hard jet, respectively; the latter gets contributions both from the hadronization and the decay of the c-quark. The p_T^μ spectrum is very steep, as explained above; we expect essentially no events with $p_T^\mu > 10\,\text{GeV}$. In contrast, the jet energy spectrum is quite hard. Obviously requiring a well-defined jet with $E_{\text{jet}} > 8$–$10\,\text{GeV}$ would not reduce our signal much. Notice that here the resolved photon contribution leads to a harder spectrum, even though its transverse momentum spectrum is softer. The reason is that the direct contribution prefers y_{jet} close to zero, so that E_{jet} is not much bigger than p_T^{jet}; in contrast, the resolved photon contribution is peaked at negative rapidities, i.e. small jet angles and hence larger jet energies for a given p_T^{jet}.

As already discussed in Sect. 2, HERA will most likely not be able to measure b-quark distribution functions. This might, however, be possible at the LEP × LHC collider. In Fig. 4a, b we show the p_T-spectrum and rapidity distribution of the photon in $b + \gamma$ events at this collider. We see that the total rate is now clearly dominated by resolved photon contributions. The reason is that a photon, when probed with sufficiently large Q^2 (our requirement $p_T^\gamma > 15\,\text{GeV}$ implies $Q^2 > 225\,\text{GeV}^2$), develops a hard, valence-like b-quark density, although it is almost 4 times smaller than the c-quark density even at asymptotically large Q^2, due to the smaller charge of the b-quark. On the other hand, the b-quark density inside the proton has to be created from gluon splitting, and is therefore confined to the region of small x_p. Furthermore, due to the much weaker Q^2 dependence of nucleon structure functions compared to photon structure functions, the b-quark density inside the proton remains much smaller and softer than the c-quark density for all values of Q^2 that are relevant for us. As a result, the direct contribution becomes essentially negligible for $y_\gamma < -2$, so that this region can be used directly for a determination

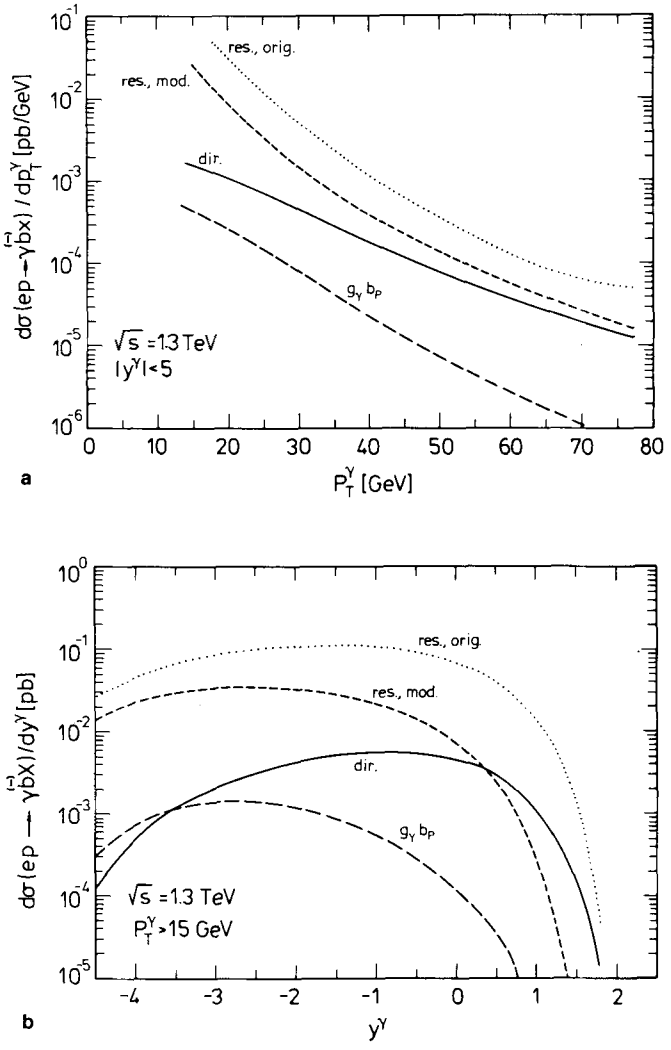

Fig. 4 a, b. The transverse momentum **a** and rapidity **b** distribution of the photon in $\gamma + b(\bar{b})$ events at LEP × LHC. Parameters and notation are as in Fig. 2, except that we have used $N_f = 5$ active flavors and EHLQ1 structure functions everywhere, since the DO1 parametrization does not include a nonzero b-quark density

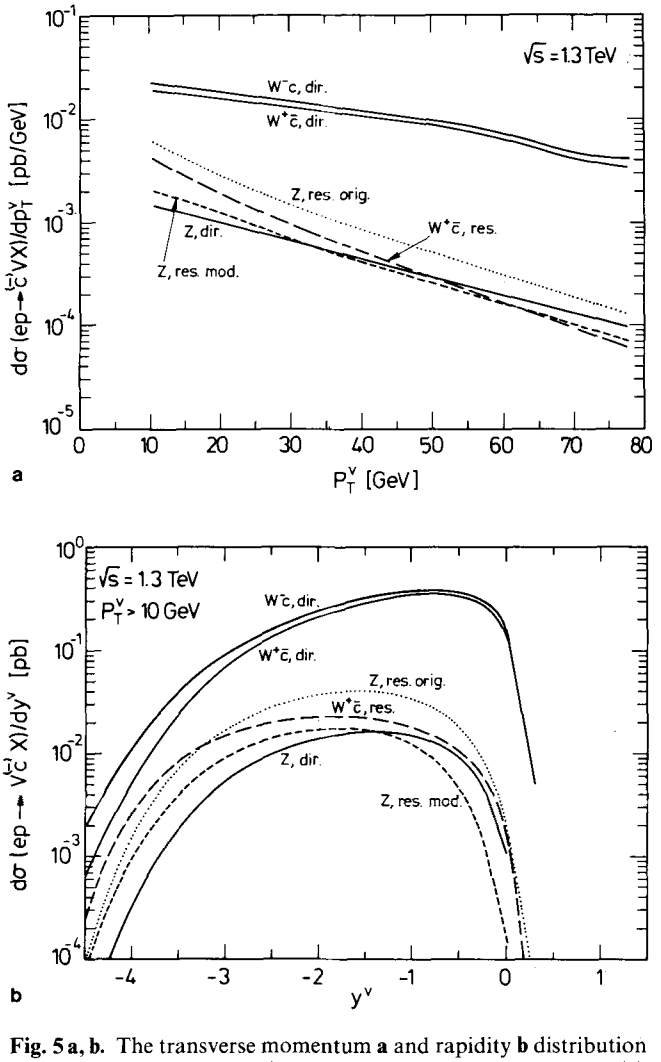

Fig. 5 a, b. The transverse momentum **a** and rapidity **b** distribution of the heavy vector boson in $V + c(\bar{c})$ events at LEP × LHC, with $V = W^+$, W^- or Z^0. The solid curves show, from top to bottom, direct contributions to cW^-, $\bar{c}W^+$, and $Z + c(\bar{c})$ production. The dotted and lower dashed curves show the resolved photon contribution to $Z + c(\bar{c})$ production, where the original and modified DG parametrization has been used, respectively. The upper dashed curves show the resolved photon contribution to $\bar{c}W^+$ production, which is not affected by the modification of (2.4), and is almost identical to the resolved photon contribution to cW^- production. We have used EHLQ1 structure functions for the proton everywhere

of the b-quark density inside the photon, without having to impose further conditions on the event (like a detectable spectator jet from the photon); notice that the contribution from the gluon inside the photon is again totally negligible. On the other hand, extracting the direct signal from the resolved photon 'background' might be more difficult here than in the case of $\gamma + c$ production at HERA.

So far we have not specified how to detect the b-quarks. Using their semileptonic decays might now be problematic, due to the c-quark background, whose cross section before cuts is at least 20 times bigger, for given p_T^γ, than the b-quark signal. This background will have a somewhat softer muon spectrum, due to the softer fragmentation function of the c-quark, but this alone will not be enough to compensate for this factor of 20. A very efficient b-quark tagging using a microvertex detector and global event shape variables seems to be necessary to extract this signal.

4 The $W, Z + c$ final states

We now turn to the associate production of heavy vector bosons and heavy quarks. We have already seen in Sect. 2 that at HERA the cross sections for these reactions are too small to be useful. Even at the LEP × LHC collider one can only study the case where the heavy quark is a c-quark. $W + b$ production is strongly suppressed by the V_{ub} and V_{cb} elements of the CKM matrix, while $Z + b$ production suffers from the smallness of the b-quark distribution functions.

In Fig. 5a, b we show the transverse momentum and rapidity distribution of the heavy boson that is produced in association with a c (anti-)quark. Notice that we do

not require either the boson or the quark to decay leptonically; most probably at least one of these requirements would have to be imposed in order to get rid of QCD backgrounds. We therefore conclude that only the direct $W+c$ production (upper solid curves) occurs with a rate that allows for a detailed investigation. In one year of running, corresponding to $10^3\,\mathrm{pb}^{-1}$, we except up to 1000 events each in the $\bar{c}W^+$ and cW^- final states, see Table 3. This is [8] about 5 times the *total* W production rate at HERA. If we tag the c (anti-)quark via its muonic decay, the rate for our reaction would be too small to significantly improve the bounds on new $WW\gamma$ couplings [25] if no signal is observed in the $W+$jet sample. However, if a signal were found, our final state might serve as statistically independent confirmation of the effect. Notice that due to the hard p_T spectrum shown in Fig. 5a, c-tagging via muons should be much more efficient here than for the $\gamma+c$ final state.

If no evidence for non-standard $WW\gamma$ couplings is found, direct $W+c$ production can provide us with important information on quark distribution functions. The total rate is dominated by contributions with an s (anti-)quark in the initial state; this explains the large differences in Table 3 for the predicted rates between the DO1 parametrizations, which assumes an $SU(3)$ flavor symmetric sea, and the EHLQ1 parametrization, which does not. Low-energy neutrino data [26] already favor $s<\bar{d}$, but these experiments are plagued [27] by uncertainties related to the proper treatment of the c-threshold. Moreover, our process could provide us with a fairly direct measurement of the shape of the s-quark distribution function inside the nucleon, from the rapidity distribution of Fig. 5b. (In contrast, non-standard $WW\gamma$ couplings would mostly affect the p_T-distribution.)

Finally, the *difference* between the cross sections for cW^- and $\bar{c}W^+$ production would be a direct measure of the valence d-quark distribution, since all other contributions cancel exactly. Other methods (like measuring [5] the W asymmetry at the tevatron, or measuring F_2^n/F_2^p in deep-inelastic scattering [28]) only measure the ratio of u- and d-quark valence distributions. Unfortunately, in our case the d-quark contribution is suppressed by a factor $|V_{cd}|^2\approx 0.05$. The difference between the total cW^- and $\bar{c}W^+$ cross sections is therefore expected to be only about 5% of the sum; one would thus need at least $5\cdot 10^3\,\mathrm{pb}^{-1}$ of data to measure it with 2σ significance, if we allow for a reduction factor of 10 for our signal after c-quark tagging and W identification. Figure 5b shows that the difference becomes larger in the region of large, negative y, which corresponds to large values of x_p; it might therefore be possible to increase the statistical significance somewhat by imposing cuts on the rapidities of the W and/or the c-quark.

The resolved photon contribution to $W+c$ production as well as the total $Z+c$ cross section are too small to use these reactions for measuring structure functions, unless the luminosity of the machine can be increased by an order of magnitude. However, even with the nominal luminosity they should at least be measurable, and can thus provide independent checks on the overall validity of our picture. Furthermore, if the Z decays into $\nu\bar{\nu}$ the $Z+c$ final state is a background for leptoquarks that decay into $c+$ neutrino, as well as for the supersymmetric production of charm-squark + sneutrino if the sneutrino is stable or decays invisibly. Figure 5a shows that this background extends to fairly large values of p_T^{miss}; adding direct and resolved contributions as well as c and $\bar{c}$ final states, we expect 7–15 (2–4) events with $p_T^{\mathrm{miss}}>20$ (50) GeV, where the uncertainty reflects our present lack of knowledge of heavy quark distribution functions.

Note that direct and resolved photon processes make quite similar contributions to $Z+c$ production, while direct processes dominate $W+c$ production by a factor of ten or more. The reason is that these last processes can proceed via the d- or s-quark content of the proton, which is still fairly hard, while direct $Z+c$ production involves the very soft c-quark density inside the proton. For the resolved photon processes the situation is reversed: $Z+c$ production involves the c-quark density of the photon which, due to the charge of the c-quark, is bigger than the s-quark density, which is relevant for resolved $W+c$ production, even if the c-quark density is modified according to (2.4). This compensates at least partly the suppression of the Z cross section due to the smaller couplings and larger mass of the Z boson, as compared to the W bosons. In addition, direct $W+c$ production is enhanced by the diagram containing the $WW\gamma$ vertex. We see from (2.6) that in the relevant limit $|\hat{t}|\ll\hat{s}$ the cross section for the direct process is proportional to the squared charge of the outgoing quark; the cross section for the resolved photon process is proportional to the squared charge of the incoming quark, because the relevant quark density inside the photon at large x contains this factor. (Recall that resolved photon contributions dominantly have the initial-state quark from the photon and the gluon from the proton.) This gives an additional relative enhancement factor of 4 for direct $W+c$ production; note that this factor depends on the details of the $WW\gamma$ vertex. Nevertheless the resolved photon contributions to W production are not negligible, since they are of the same order as the direct contributions from the d-quarks inside the proton.

5 Summary and conclusions

In this paper we have studied the reactions $ep\to eQVX$, where Q stands for a c or b quark and V is an *isolated* photon or a W or Z boson. In Sect. 2 we discussed the necessary formalism, including an ansatz [17] for the heavy quark distribution functions inside the photon. We then presented total cross sections after cuts for HERA ($\sqrt{s}=314\,\mathrm{GeV}$) and the LEP × LHC collider ($\sqrt{s}=1.3\,\mathrm{TeV}$); our results are summarized in Tables 1–3. We found that at HERA only the combination $V=\gamma$, $Q=c$ is promising, while at LEP × LHC all $V+c$ final states as well as the $\gamma+b$ final state should have at least detectable event rates.

In Sect. 3 we therefore focussed on the $\gamma+Q$ final states. We found that HERA has a good chance to measure both the shape and the normalization of the c-quark distribution functions both in the proton and in the photon; at present, these are only known up to a factor of 2 or so. However, this potential can only be

fully exploited if direct and resolved photon contributions can be distinguished on an event-by-event basis; this will probably only be possible if one can tag on or against the spectator jet from the initial-state photon which exists only in resolved photon events. Furthermore, one will have to be able to identify muons with tansverse momentum down to 3, or better even 2 GeV.

Clearly the rate for $\gamma + c$ production at HERA will be much lower than at the Tevatron or even the SpS collider. However, at these colliders the rate depends both on the gluon and on the c-quark density inside the proton, neither of which is known accurately. Therefore $\gamma + c$ production at hadron colliders [6] by itself can only serve as important constraint on, but not direct measurement of, parton distribution functions. In contrast, direct $\gamma + c$ production at ep colliders can determine the c-quark density inside the proton directly, since the photon flux inside the electron is computable unambiguously in QED.

LEP $\times$ LHC will be a very copious source of $\gamma + c$ events. While this will allow one to study this final state in great detail, it might make it difficult to study the $\gamma + b$ final state, whose cross section is some 20 times smaller. The detection of this latter final state puts even more stringent requirements on b-quark identification than the search [21] for an intermediate mass Higgs boson at this collider. Finally, we saw that measurements of $W + c(\bar{c})$ production would in principle allow one to determine the strange sea and the valence d-quark distribution inside the proton, although with the foreseen luminosity of $10^3\,\mathrm{pb}^{-1}$ per year the latter measurement will take more than one year if one has to tag c-quarks via their muonic decays. It should be noted, however, that a detector that allows for a very efficient b-quark tagging also enables one to distinguish between hadronically decaying c-quarks on the one hand and light quarks and gluons on the other.

We conclude that ep colliders offer unique opportunities to measure heavy quark densities both inside the proton and inside (quasi-)real photons. On the one hand, this might improve our understanding of QCD; e.g., the old question [29] of an "intrinsic charm" in the nucleon will be settled unambiguously. On the other hand, heavy quark distributions in the proton make increasingly important contributions to a variety of processes as the energy of hadron colliders increases. Already now the lack of knowledge of the c-quark density considerably increases [30] the error on the W decay width as extracted from the measurement of the ratio of events with leptonically decaying W and Z bosons at the tevatron. Eventually the uncertainty in structure functions might also limit the precision with which the W mass can be measured at hadron colliders. Finally, at pp supercolliders $b\bar{b}$ and $b\bar{c}$ annihilation can be [31] important sources of non-standard neutral and charged Higgs bosons. We therefore think that an experimental study of our reactions, although perhaps not easy, is well worth the effort.

Acknowledgements. One of us (C.S.K.) would like to thank the DESY theory group for their hospitality. The work of C.S.K. was supported by the Science and Engineering Research Council, U.K.

References

1. For a review, see: J.F. Owens: Rev. Mod. Phys. 59 (1987) 465
2. UA1 collab.: C. Albajar et al.: Z. Phys. C – Particles and Fields 44 (1989) 15; UA2 collab.: J. Alitti et al.: Z. Phys. C – Particles and Fields 47 (1990) 11
3. CDF collab.: F. Abe et al.: Fermilab report PUB-90-229-E
4. S.L. Glashow: Nucl. Phys. B22 (1961) 579; S. Weinberg: Phys. Rev. Lett. 19 (1967) 1264; A. Salam: in: Elementary particle theory. Nobel Symposium No. 8, N. Swartholm (ed.) Stockholm: Almqvist & Wiksell 1968
5. S. Leone for the CDF collab.: Talk presented at the 26th Rencontres de Moriond on Electroweak Interactions and Grand Unified Theories, Les Arcs, 1991; See also: E.L. Berger, F. Halzen, C.S. Kim, S.S.D. Willenbrock: Phys. Rev. D40 (1988) 83 and erratum: D40 (1988) 3789
6. R.S. Fletcher, F. Halzen, E. Zas: Phys. Lett. B221 (1989) 403
7. C.S. Kim, A.D. Martin, W.J. Stirling: Phys. Rev. D42 (1990) 952; C.S. Kim: Nucl. Phys. B353 (1991) 87
8. K.O. Mikaelian: Phys. Rev. D17 (1978) 750; H. Neufeld: Z. Phys C – Particles and Fields 17 (1983) 145; G. Altarelli, G. Martinelli, B. Mele, R. Rückl: Nucl. Phys. B262 (1985) 204; E. Gabrielli: Mod. Phys. Lett. A1 (1986) 465; M. Drees: Mod. Phys. Lett. A2 (1987) 573; U. Baur, D. Zeppenfeld: Nucl. Phys. B325 (1989) 253
9. A.C. Bawa, W.J. Stirling: J. Phys. G14 (1988) 1353; M. Krawczyk: Acta Phys. Pol. B21 (1990) 999; A.C. Bawa, M. Krawczyk, W.J. Stirling: Z. Phys. C – Particles and Fields 50 (293) 1991; A.C. Bawa, M. Krawczyk: Phys. Lett. B262 (492) 1991
10. C.F.v. Weizsäcker: Z. Phys. 88 (1934) 612; E.J. Williams: Phys. Rev. 45 (1934) 729
11. A.C. Bawa, W.J. Stirling: J. Phys. G15 (1989) 1339
12. D.W. Duke, J.F. Owens: Phys. Rev. D30 (1984) 49
13. E.J. Eichten, I. Hinchliffe, K.O. Lane, C. Quigg: Rev. Mod. Phys. 56 (1984) 579
14. E. Witten: Nucl. Phys. B120 (1977) 189
15. M. Drees, K. Grassie: Z. Phys. C – Particles and Fields 28 (1985) 451
16. R.J. DeWitt et al.: Phys. Rev. D19 (1979) 2046
17. C.S. Kim: Univ. Durham Report DTP/91/06
18. PLUTO collab.: Ch. Berger et al.: Nucl. Phys. B281 (1987) 365; TASSO collab.: M. Althoff et al.: Z. Phys. C – Particles and Fields 31 (1986) 527; AMY collab.: T. Sasaki et al.: Phys. Lett. B252 (1990) 491
19. For a review, see: E.A. Paschos, U. Türke: Phys. Rep. 178 (1989) 145
20. C. Peterson, D. Schlatter, I. Schmitt, P. Zerwas: Phys. Rev. D27 (1983) 105
21. G. Grindhammer et al.: in the Proceedings of the Large Hadron Collider Workshop, Aachen, 1990, CERN Yellow Book 90-10, Vol. II
22. M. Drees, R.M. Godbole: Nucl. Phys. B339 (1990) 355
23. A.D. Martin, R.G. Roberts, W.J. Stirling: Phys. Rev. D37 (1988) 1161
24. M. Drees, R.M. Godbole: Phys. Rev. D39 (1989) 169
25. U. Baur, B.A. Kniehl, J.A.M. Vermaseren, D. Zeppenfeld: In [21]
26. W.H. Smith for the CCFR collab.: Talk presented at the Neutrino 90 conference, CERN, 1990
27. M.A.G. Aivazis, F.I. Olness, W.-K. Tung: Phys. Rev. Lett. 65 (1990) 2339
28. EMC collab.: J.J. Aubert et al.: Nucl. Phys. B259 (1985) 189; BCDMS collab.: A.C. Benvenuti et al.: Phys. Lett. B223 (1989) 485
29. S.J. Brodsky, P. Hoyer, C. Peterson, N. Sakai: Phys. Lett. B93 (1980) 451
30. K. Hagiwara, F. Halzen, C.S. Kim: Phys. Rev. D41 (1990) 1471
31. See e.g.: D.A. Dicus, S.S.D. Willenbrock: Phys. Rev. D39 (1989) 751